A Deep Learning Based on Sparse Auto-Encoder with MCSA for Broken Rotor Bar Fault Detection and Diagnosis

SEGHIOUR Abdellatif[a], CHOUDER Aissa[b], AIT ABBAS Hamou[c], SALMI Chawki[d], BEN SAADIA Oussama[e]

[a]Ecole Supérieur en Génie Electrique et Énergétique d'Oran
[b]Electrical Engineering Laboratory (LGE), University Mohamed Boudiaf of M'sila, BP 166, 28000, Algeria
[c]Laboratoire d'informatique, Mathématique et Physique pour l'agriculture et les Forets, University of Bouira, Algeria
[d]Laboratory of Instrumentation, University of Sciences and Technology Houari Boumediene, BP 32 EL ALIA, BAB EZZOUAR, Algeria.
[e] Electrical Engineering Faculty, Diagnosis Group University of Sciences and Technology of Oran Oran, Algeria
Emails : seghiour.abdellatif@gmail.com

***Abstract*—The understanding of the Broken Rotor Bar (BRB) features frequencies and amplitudes has a great importance for all diagnostic methods. These characteristics frequencies shows a drawbacks under varying load condition. The discrete Fourier transform (DFT) has been widely used to achieve these requirements, because of its efficiency. However, this paper present an enhancing of the fault detection based on a Machine Current Signature Analysis (MCSA) method. Indeed, the use of Sparse Autoencoder (AE) with the combination of Multi-Layer Perceptron (MLP) shown a good accuracy. Furthermore, the extraction of the new features to use in multi-class classification for the healthy and faulty Induction Motor (IM) is presented.**

***Index Terms*—Deep Learning, Sparse Auto-Encoder Machine Current Signature Analysis, Fault Diagnosis and Detection, Broken Rotor Bar, Induction Motor.**

I. Introduction

Three phase IMs are widely used in industry. Their applications are many and consumers are attracted to them for their reliability and good design. IMs are classified into two main types based on their rotors: squirrel cage and wound rotor (slip-ring). They produce a good range of starting torque, ranging from medium to high starting torque [1]. However, the diagnostic system must include a robust fault detection, which allows detecting all faults or any imperfections changes on the motor performances before a total failure occurrence [2].

The MCSA has been widely used to detect BRBs in an IMs [3]. It is well known that BRBs produce geometric and magnetic unbalances which induce sidebands [4], $(1 \pm 2ks)f_s$, in the stator current spectrum, where f_s is the supply frequency and s is the motor slip. Therefore, the identification of the sideband frequencies and the evaluation of their amplitudes can be used as an efficient and reliable approach to diagnose rotor bar faults. Meanwhile, these sidebands are usually quite close to the fundamental frequency, and they may become sensitive to load variations. In addition, the magnitudes of the sideband components are in the range of -20 to -60 dB under the magnitude of the fundamental, which, combined with the noise usually present in the signal, makes the task of separating the different harmonic frequencies difficult, and consequently, the harmonic estimation is still an open research topic [1].

Artificial Neural Networks (ANNs) are parallel data-processing tools capable of learning functional dependencies of the data and have been used in fault diagnosis of various components [5]. However, there are relatively few historical studies for the detection of multiple simultaneous faults using ANNs [6].

Under these circumstances, the present paper develop a technique based on the use of the unsupervised learning for an Autoencoder neural network. An AE is a three Layer neural neural network which containing an input is the same output in addition a hidden layer [7].

This technique is used to extract a new features that can stacked all each other. However, the sidebands around the fundamental frequency is used as an input, the output of deep neural network represented the status of the machine.

The next paragraph explained how a deep neural network works. The fundamental trick in deep learning is to use this score as a feedback signal to adjust the value of the weights a little, in a direction that will lower the loss score. This adjustment is the job of the optimizer, which implements what's called the Backpropagation algorithm: the central algorithm in deep learning [8].

The contribution of the present paper is to develop a technique based on the deep learning method to achieve the detection of BRBs in an IM as fellows :

- Step 1: collect the data from the model of healthy and faulty IM.
- Step 2: Pre-train the two-layer AE per layer.
- Step 3: Pre-train the MLP classifier : Use a MLP model to classify the final result using the new features as input, and obtain the pre-trained MLP classifier.

978-1-5386-4988-6/18/$31.00 ©2018 IEEE

- Step 4: Establish the deep neural network: Establish a three-layer deep neural network, and assign first two layer's weights using the pre-trained AE (W^1, W^2), and assign the last layer using the pre-trained MLP classifier.
- Step 5: Fine-tune the deep neural network.
- Step 6: Output the results: After training the neural network, output the structure and the prediction.

II. Modeling and Simulation an IM under Normal and Faulty State

In order to create the full dynamic model to describe the behaviour of an IM, in specific, the coupling inductances have to be embedded into suitable supply voltage equations. This approach will require the coupling inductances: stator – stator; stator – rotor; rotor – stator; and rotor - rotor. It will relate the terminal voltages to the currents in the stator and rotor as both time and speed change. The mathematical dynamic model that represents a cage rotor IM is a set of simultaneous first-order initial value ordinary differential equations.

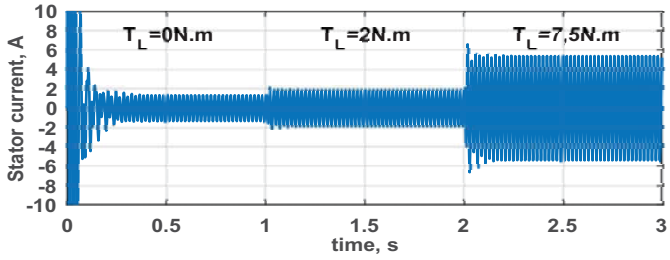

(a) Healthy motor

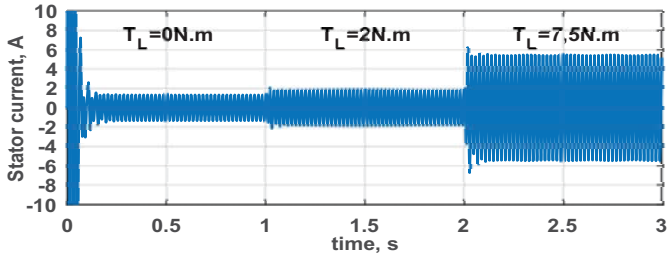

(b) Motor under 2 BRBs

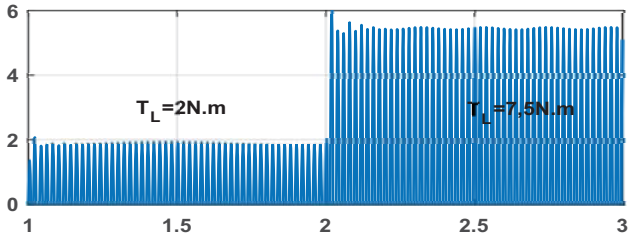

(c) Zoom of Fig.1b

Figure 1: Variable Load Stator Current motor under healthy and faulty states.

The final dynamic harmonic model that represents the behaviour of a cage IM is initially rearranged as a standard first order differential equation. The preferred numerical method to solve this initial condition first order ODE is a $RungeKutta^{4th}$ order method. The full electro-mechanical dynamic equations are rearranged in the following form [9]

$$\begin{aligned}&\tfrac{d}{dt}\left[\begin{array}{cccccccccccc} I_a & I_b & I_c & I_{r_1} & I_{r_2} & I_{r_3} & . & . & . & I_{r_n} & I_e & \omega_r & y_m \end{array}\right]^T = \\ &[b]^{-1}\left[\left[\begin{array}{cccccccccccc} V_a & V_b & V_c & V_{r_1} & V_{r_2} & V_{r_3} & . & . & . & V_{r_n} & V_e & \frac{(T_e-T_l)}{J_e} & \omega_r \end{array}\right]^T \right. \\ &\left. -[a]\left[\begin{array}{cccccccccccc} I_a & I_b & I_c & I_{r_1} & I_{r_2} & I_{r_3} & . & . & . & I_{r_n} & I_e & \omega_r & y_m \end{array}\right]^T\right]\end{aligned} \tag{1}$$

where $[a] = \begin{bmatrix} [R_s] & [G_{rs}] & [0] \\ [G_{sr}] & [R_r] & [0] \\ [0] & [0] & [0] \end{bmatrix}$ and $[b] = \begin{bmatrix} [M_{ss}] & [M_{rs}] & [0] \\ [M_{sr}] & [M_{rr}] & [0] \\ [0] & [0] & \begin{bmatrix} 1 & 0 \\ 0 & 1 \end{bmatrix} \end{bmatrix}$

Fig. 1, 2 and 3 shows the quasi-steady state instantaneous values of IM at three different load levels ($T_L = 0, 2$ and $7.5N.m$) for normal and faulty conditions under balanced sinusoidal voltage supply. Fig. Fig. 1(a)–(c) show three phase stator currents. Fig. 2(a) and (b) show the torque variables. Fig. 3(a) and (b) show the speed.

The initial transient stator current shown in Fig. 1 simply represents the input current during the motor run-up to synchronous speed. Moreover, after the second one multiple torque has applied as has been seen. As expected the results from the dynamic model and the per-phase equivalent circuit are closely identical. the dynamic model starts initially with a no-load run-up. The full load torque $7.5N.m$ is applied at $2s$ seconds. From Fig.1 , the peak stator current for one of the phase windings is $5.9A$.

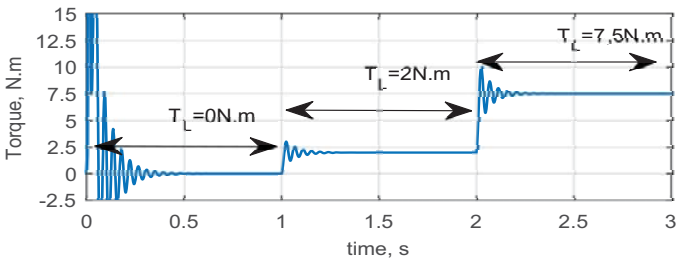

(a) Healthy motor

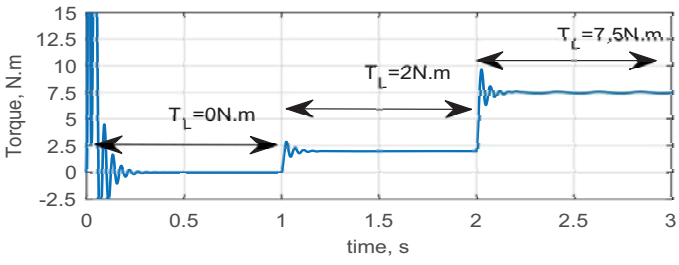

(b) Motor under 2 BRBs

Figure 2: Variable Load Torque motor under healthy and faulty states.

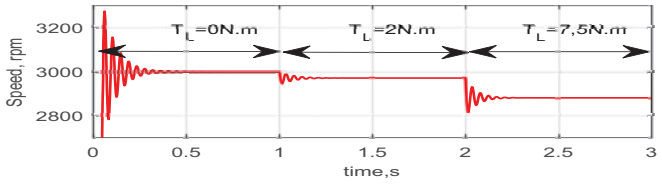

(a) Healthy motor

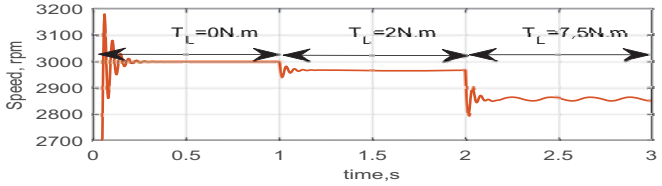

(b) Motor under 2 BRBs

Figure 3: Variable Load Rotor Speed motor under healthy and faulty states,(a) Healthy motor (b) under 2 BRBs.

The results depicts that load level varying itself leads to stator current and torque increase and rotor speed decrease. The amplitude of stator current increases from 0.6 at no load to 5.9 at full load. In contrast to stator current incensement, rotor speed changes from 2988 at no load to 2760 at full load.

These figures clearly show that the fault extent and load level play a fundamental role in the amplitude variation of the motor variables. More specifically, load level changes cause motor variable amplitude constant alteration as shown. In contrast to this, in Figs. 1, 2 and 3, broken bar fault extent changes have a direct impact to the ripples of motor signals and this impact including both amplitude and frequency.

The values of the sideband frequencies and amplitudes are the parameters of interest for IM broken rotor bar detection. The results depicted in Fig. 4 clearly show the changes that happened on the frequencies and amplitudes after the occurrence of the rotor fault.

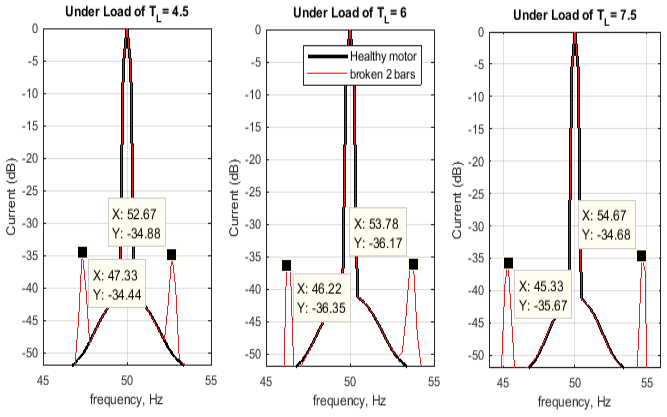

Figure 4: Current spectrums of healthy and faulty states of motor under varying load condition.

In order to enhance the fault detection this paper is propose a sparse autoencoder to extract a new features based on the sideband components of the stator current spectrum. the next section discuss this approach.

III. Deep Learning

Deep learning (DL) enables computational models that consist of multiple processing layers to learn representations of data with multiple levels of abstraction. These methods have dramatically improved the fault detection. Due to the lack of proper training algorithms a two step procedure is proposed to train the deep neural network as follows:

- Initialization of weights using greedy layer-wise unsupervised learning algorithm as the autoencoder.
- Using supervised data, fine-tuning of the previously intialized weights to provide better classification.

A. Autoencoder

An autoencoder is a three-layer network containing an encoder and a decoder. Fig.5 shows the general structure of an autoencoder neural network. The encoder maps the input data from a high-dimensional space into codes in a low-dimensional space, and the decoder reconstructs the input data from the corresponding codes [7].

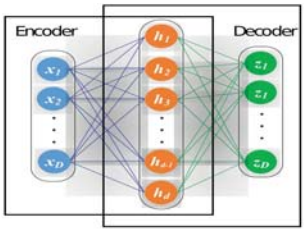

Figure 5: The structure of an autoencoder.

Given the training samples $x = \{x_1, x_2, ...x_m\}$ (for each sample x_i , $x_i = [x_1, x_2, ...x_D]^T$), the encoder transforms the input vector x into a hidden representation $h = \{h_1, h_2, ...h_m\}$ (for each , $h_i = [h_1, h_2, ...h_d]^T$) through the sigmoid function as follows:

$$h = s_f\left(W^{(1)}x + b^{(1)}\right) \tag{2}$$

$$s_f(t) = 1/\left(1 + e^{-t}\right) \tag{3}$$

where x and h are D-dimensional and d-dimensional vectors, respectively, $W^{(1)}$ is a $d\times$D$-$dimensional weight matrix and $b^{(1)}$ is a $d - dimensional$ bias vector.

Then, the vector h is transformed back to a reconstruction vector $z = \{z_1, z_2, ...z_m\}$ (for each z_i , $z_i = [z_1, z_2, ...z_D]^T$) by the decoder as follows:

$$z = s_f\left(W^{(2)}h + b^{(2)}\right) \tag{4}$$

where z is a D$-$dimensional vector, $W^{(2)}$ is $D\times$d$-$dimensional weight and $b^{(2)}$ is a D$-$dimensional bias vector. The autoencoder training aims to optimize the parameter set $\theta = \left\{W^{(1)}, b^{(1)}, W^{(2)}, b^{(2)}\right\}$ minimizing the

reconstruction error. The mean square error (MSE) is usually used as the standard autoencoder loss function [7].

$$J_{MSE}(\theta) = \frac{1}{m}\sum_{i=1}^{m} L_{MSE}(x_i, z_i) = \frac{1}{m}\sum_{i=1}^{m}\left(\frac{1}{2}\|x_i - z_i\|^2\right) \tag{5}$$

Considering the advantages of sparse inputs in learning useful features, in this work, we regularize the loss function by a sparsity term defined as [7].

$$J_{sparse}(\theta) = \beta\sum_{j=1}^{s_2} KL(\rho\|\hat{\rho}_j) \tag{6}$$

$$\hat{\rho}_j = \frac{1}{m}\sum_{i=1}^{m}\left[a_j^{(2)} x_i\right] \tag{7}$$

$$KL(\rho\|\hat{\rho}_j) = \rho\log\frac{\rho}{\hat{\rho}_j} + (1-\rho)\log\frac{1-\rho}{1-\hat{\rho}_j} \tag{8}$$

where β is the weight adjustment parameter, s_2 is the number of units in the second layer, $\hat{\rho}_j$ is the average activation value for the ith hidden layer unit, and ρ is a sparse parameter.

In addition, a weight decay term $J_{weight}(\theta)$ is also added to avoid overfitting expressed as :

$$J_{weight}(\theta) = \frac{\lambda}{2}\sum_{l=1}^{2}\sum_{i=1}^{S_l}\sum_{j=1}^{S_{l+1}}\left(w_{ij}^{(l)}\right)^2 \tag{9}$$

where $w_{ij}^{(l)}$ is an element in $W^{(l)}$, λ is the parameter to adjust the weight of $J_{weight}(\theta)$, and s_l is the number of units in layer l. We define the autoencoder loss function as:

$$E(\theta) = J_{MSE}(\theta) + J_{weight}(\theta) + J_{sparse}(\theta) \tag{10}$$

By now, the deep autoencoder is designed as shown in the Fig. 6, where the sidebans lower and upper components of stator current spectrum are used as an input of the first autoencoder. Moreover, the second autoencoder is used to extract the new feature to use in the classification step of healthy and faulty IM under one and two BRBs. The next step is to optimize the deep autoencoder parameters for deep learning and fault diagnosis.

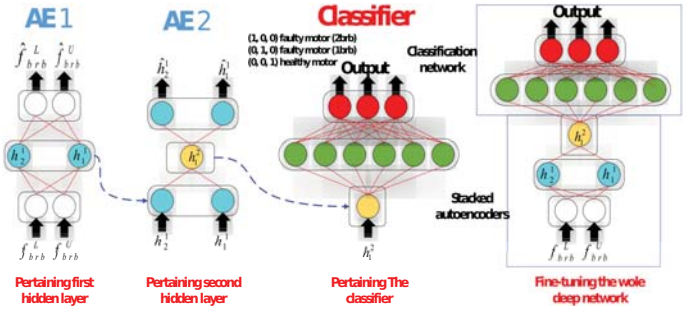

Figure 6: A deep architecture of the proposed autoencoder and two step parameter optimization scheme.

B. Unsupervised fault characteristic deep learning with sparse representation

A problem usually arises in the deep learning process when the variation load is applied that cannot be ignored is mixed within the stator current spectrum, which is hard to deal with manually because of the varying slips affected to the samples to be trained. In this paper, the select data set is collected through simulations by Matlab, under different operating conditions of the IM [10], [11]. The data is composed by a successive range of 54 samples representing three states of the operating conditions of the IM under varying load conditions (T_L = 1 to 10 $N.m$) as follow:

- Healthy machine(18 samples);
- One broken bar (18 samples);
- Two broken bars (18 samples).

The NN has three binary output ($Out_{NN_{1,2,3}}$ are the Target) to indicate the state of an IM as flows:

- $if \rightarrow Out_{NN_{1,2,3}} = (1,0,0)$: Two broken bars;
- $if \rightarrow Out_{NN_{1,2,3}} = (0,1,0)$: One broken bar;
- $else \rightarrow Out_{NN_{1,2,3}} = (0,0,1)$: Healthy state.

However, the original input is still used as the target for the reconstruction in the deep learning process. The autoencoder is thus applied for the following feature reconstruction based on the unsupervised learning process mentioned above. Note that the data destruction process is conducted in all layers of the autoencoder model instead of only the input layer. The destruction process of each layer during signal processing is shown in Fig.2

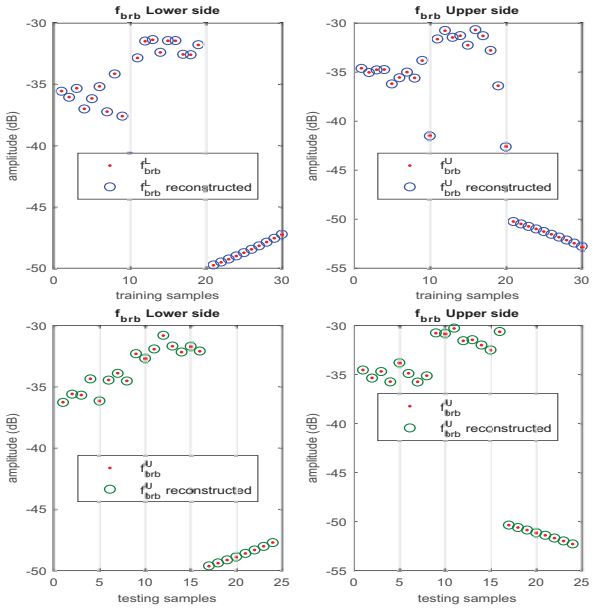

Figure 7: Destruction process for the input training and testing data in each layer.

Based on the obteined results is very clear that the both of training and testing are well reconstructed. The next step is to use the vector of the hidden layer h_1^1 and h_2^1 for the

unsupervised training in the next autoencoder as shwon in Fig.6 to extract the new features.

The Fig.8 shows the new features for the input training and testing data. Indeed, the results shows a well representation which can see the separated data between healthy and faulty state.

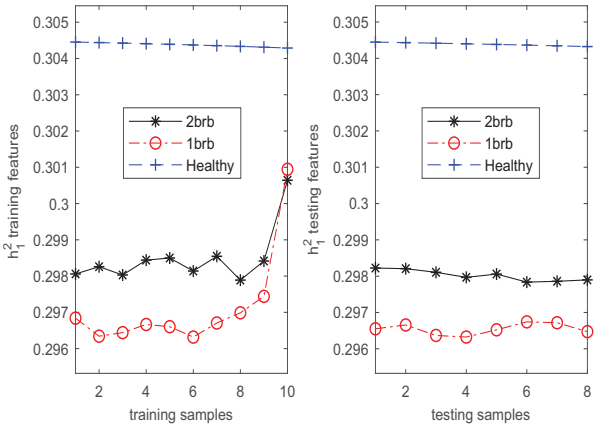

Figure 8: The new features for the input training and testing data.

The desired of the training and testing outputs of NN are shown in Figs. 9, 10 and 11. The training errors are very low, proving that the NN has well learned the input data and has correctly reproduced the desired output.

IV. Fault Detection and Diagnosis Results

In this section we present a comparative simulation results of a normal MLP and stacked autoencoder with MLP. To address the health state identification problems effectively with the AE, the first step is to identify the data format and diagnosis targets. Pre-processing is then conducted as the second step based on the data requirements to ensure both the diagnosis accuracy and the computational efficiency. Pre-processed data are divided into training and testing groups consisting of a series of batches for forward and back propagation learning. The architecture parameters of the AE are initialized with small random values, and distinct updates are calculated and integrated as diverse parts of the full deep network. The number of loops for the unsupervised learning and back propagation process is determined by the maximum number of epochs set for the model. Finally, the faulty and healthy are classified with high accuracy, which are compared with a classical MLP.

A. MLP network classification

Fig.'9 is shown the use of the sideband frequency (f_{brb}^{U} and f_{brb}^{U}) as an input to the MLP classify. This result shown a poor detection and misclassification is included mainly due to the load effect and the fault. Moreover, the Fig.10 shown a good classification when we use the pretrained of the stacked autoencoder that enhance the detection.

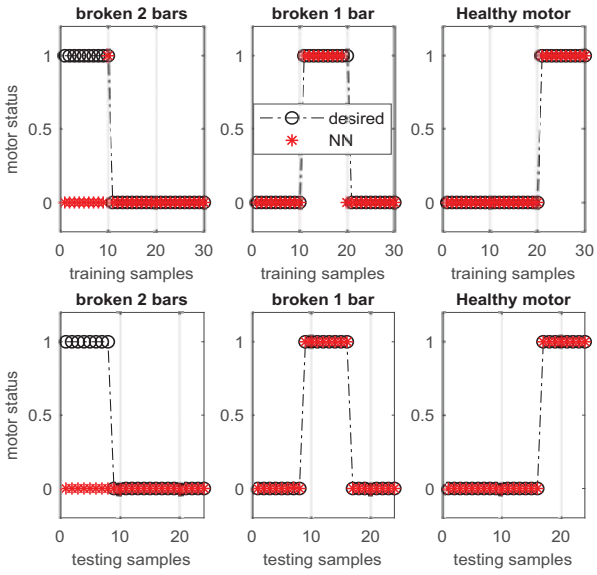

Figure 9: The Terget of NN training and testing results for a simple Classifier MLP.

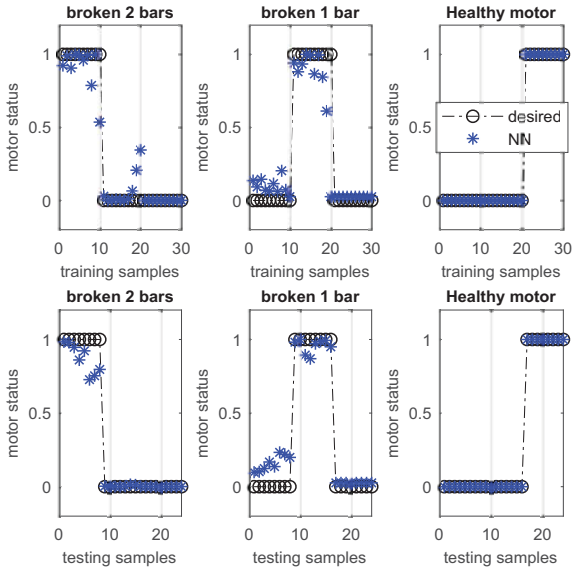

Figure 10: The Terget of NN training and testing results for the pretraining deep network.

V. Back Propagation Learning Based Fine Tuning

The parameters derived from multiple hidden layers are determined to be the input of a supervised classifier followed by the global back propagation optimization process. In this study, the MLP regression algorithm is employed for multi-class classification of healthy and BRBs. Fig.11 shows a well classification between 2 brbs, 1brb and healthy state where the fine-tuning of the whole deep network.

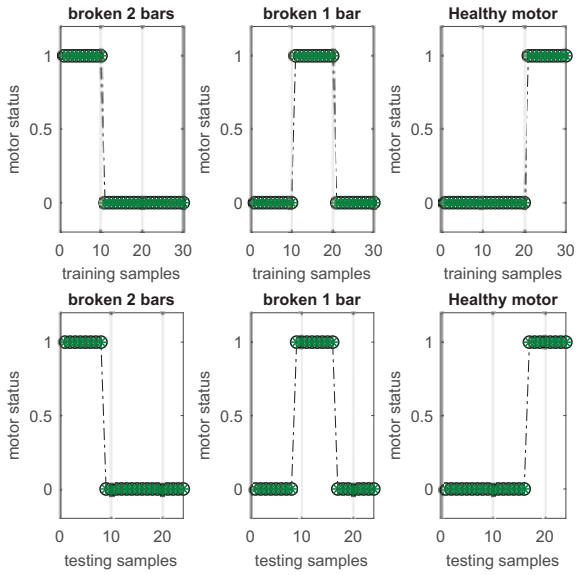

Figure 11: The Terget of NN training and testing results for the tune-train whole of the deep network..

VI. Conclusion

It has been shown that the side band current components at frequencies $(1 \pm 2ks)f_s$, generally used for rotor fault diagnosis of an IM. These characteristic frequencies are strongly dependent on the load level and fault extent. In this paper, a deep autoencoder feature learning method is proposed for rotating machinery fault diagnosis. Following the physical phenomena caused by the failure, simplified relationships that link stator current, speed and torque ripples components have been derived. Furthermore, the sidebands around the fundamentals frequency have used and enhanced based on the deep learning method. Finally, the results presents a well classification that can be used and validated experimentally future.

Appendix A

Table I: Machine parameters

Paramater	value
Number of Poles	2
Output Power	2.2 KW
Voltage	400 V
Number of Phases	3
Frequency	50 Hz
stator Winding Resistance	3.43 Ω
Number of bars	29
Machine axial length	97 mm
Air-gap mean Diameter	66.3775 mm
Number of slots	24
Winding Leakage Inductance	5.443 (mH)
Inertia	0.0028 $kg.m^2$
Effective air-gap	0.591 mm
Bar resistance	133.4 $\mu\Omega$
End-ring resistance	37 $\mu\Omega$
Bar inductance	1.08 μH
End-ring inductance	10 nH
Skew angle	0.149 rad

References

[1] A. Seghiour, T. Seghier, B. Zegnini, and G. Georgoulas, "Diagnosis of the combined rotor faults using air gap magnetic flux density spectrum for an induction machine," *International Journal of System Assurance Engineering and Management*, vol. 8, no. 2, pp. 1503–1519, Nov 2017. [Online]. Available: https://doi.org/10.1007/s13198-017-0621-9

[2] R. R. Schoen, B. K. Lin, T. G. Habetler, J. H. Schlag, and S. Farag, "An unsupervised, on-line system for induction motor fault detection using stator current monitoring," *IEEE Transactions on Industry Applications*, vol. 31, no. 6, pp. 1280–1286, 1995.

[3] J.-H. Jung, J.-J. Lee, and B.-H. Kwon, "Online diagnosis of induction motors using mcsa," *IEEE Transactions on Industrial Electronics*, vol. 53, no. 6, pp. 1842–1852, 2006.

[4] P. Karvelis, G. Georgoulas, I. P. Tsoumas, J. A. Antonino-Daviu, V. Climente-Alarcón, and C. D. Stylios, "A symbolic representation approach for the diagnosis of broken rotor bars in induction motors," *IEEE Transactions on Industrial Informatics*, vol. 11, no. 5, pp. 1028–1037, 2015.

[5] G. Georgoulas, P. Karvelis, T. Loutas, and C. D. Stylios, "Rolling element bearings diagnostics using the symbolic aggregate approximation," *Mechanical Systems and Signal Processing*, vol. 60, pp. 229–242, 2015.

[6] K. Watanabe, S. Hirota, L. Hou, and D. Himmelblau, "Diagnosis of multiple simultaneous fault via hierarchical artificial neural networks," *AIChE Journal*, vol. 40, no. 5, pp. 839–848, 1994.

[7] L. Wen, L. Gao, and X. Li, "A new deep transfer learning based on sparse auto-encoder for fault diagnosis," *IEEE Transactions on Systems, Man, and Cybernetics: Systems*, 2017.

[8] C. Lu, Z.-Y. Wang, W.-L. Qin, and J. Ma, "Fault diagnosis of rotary machinery components using a stacked denoising autoencoder-based health state identification," *Signal Processing*, vol. 130, pp. 377–388, 2017.

[9] P. Shi, Z. Chen, Y. Vagapov, and Z. Zouaoui, "A new diagnosis of broken rotor bar fault extent in three phase squirrel cage induction motor," *Mechanical Systems and Signal Processing*, vol. 42, no. 1-2, pp. 388–403, 2014.

[10] S. Abdellatif, S. Tahar, and Z. Boubakeur, "Diagnostic of the simultaneous of dynamic eccentricity and broken rotor bars using the magnetic field spectrum of the air-gap for an induction machine," in *Control, Engineering & Information Technology (CEIT), 2015 3rd International Conference on*. IEEE, 2015, pp. 1–6.

[11] A. Seghiour, T. Seghier, B. Zegnini, and G. Georgoulas, "Multi-class classification approach for the diagnosis of broken rotor bars based on air-gap magnetic flux density," *Electrotehnica, Electronica, Automatica (EEA)*, vol. 65, no. 2, pp. 31–39, 2017.